PET Imaging of Brain Tumor with [*methyl*-^{11}C]Choline

Toshihiko Hara, Noboru Kosaka, Nobusada Shinoura and Tatsuya Kondo
Departments of Radiology and Neurosurgery, International Medical Center of Japan

This article describes a new method of [^{11}C]choline synthesis for intravenous injection. We aimed at the utilization of this compound for brain tumor imaging with PET. **Methods:** After [^{11}C]carbon dioxide production in a cyclotron and the subsequent [^{11}C]methyl iodide synthesis, [*methyl*-^{11}C]choline was synthesized by the reaction of [^{11}C]methyl iodide with "neat" dimethylaminoethanol at 120°C for 5 min. Purification was achieved by evaporation of the reactants followed by passage of the aqueous solution of the product through a cation-exchange resin cartridge. The time required for overall chemical processing, excluding the cyclotron operation, was 15 min. Radiochemical yield was >98%. Radiochemical purity was >98%. Chemical purity was >90% (dimethylaminoethanol was the only possible impurity). Specific radioactivity of the product was >133 GBq/μmol. The whole body distribution was examined in rabbits with PET. Clinical studies were performed in patients with brain tumor using PET after intravenous injection of 370 MBq of [^{11}C]choline. **Results:** In rabbits, [^{11}C]choline was taken up from blood by various tissues very rapidly, and the radioactivity remaining in blood became almost negligible 5 min after intravenous injection. Taking advantage of this characteristic, we obtained stable tissue distribution images of human brain using PET. In patients with brain tumor, PET produced clearly delineated positive images of the tumors. **Conclusion:** Carbon-11-choline can be used for obtaining clear images of brain tumor in PET.

Key Words: PET; choline; brain tumors

J Nucl Med 1997; 38:842–847

The incorporation of radioactive choline from blood into acetylcholine in the brain has been a matter of great interest for many years. Contrary to the general expectation, Haubrich et al. (*1*) found in animal studies that the major radioactivity in brain and other organs measured soon after intravenous injection of [*methyl*-^{3}H]choline was not associated with acetylcholine but with phosphorylcholine, an intermediate involved in phospholipid synthesis. Friedland et al. (*2*) synthesized [*methyl*-^{11}C]choline by the reaction of [^{11}C]methyl iodide with dimethylaminoethanol (details of the method have not been reported) and examined its distribution using PET after injection in normal animals. They observed that brain uptake was very low relative to extracerebral tissues. Gauthier et al. (*3*) confirmed this phenomenon in human subjects after injection of [^{11}C]choline, but they did not pay attention to brain tumors.

Choline is incorporated into cultured mammalian cells across cell membranes at physiological choline concentration via two kinds of energy-dependent transport systems (*4*). One is present ubiquitously in all mammalian cells and is associated with phosphorylcholine synthesis. Phosphorylcholine is integrated into a major membrane phospholipid, phosphatidylcholine. Cholinergic nerve endings (synaptosomes), on the other hand, contain another kind of specific choline transport system that is tightly coupled to acetylcholine synthesis. Most normal brain cells and neurogenic tumor cells are characterized by the predominance of phosphorylcholine synthesis (*5–9*). Neuroblastoma cell lines NS20, N18 and N1E incorporate [^{3}H]choline very rapidly, and most of the radioactivity found in the cells after 4 min is in phosphorylcholine (95%–97%); very little is in acetylcholine (0.1–0.5%) or phosphatidylcholine (0.1%) (*5*). The human neuroblastoma LA-N-2 cell line is the only exception in which acetylcholine synthesis is dominant (*10*).

It is believed that circulating choline in blood penetrates at first through an amine-specific transport system of brain capillary endothelium, blood-brain barrier. The ease for choline to penetrate through the blood-brain barrier is comparable with that for neutral amino acids (*11*). Choline then penetrates through the choline-specific transport system of brain cell membranes as described above. It is not clear, however, which transport system constitutes the rate-limiting step on the net entry of choline into the brain cells.

Using nuclear magnetic resonance spectroscopy (MRS) in brain tumor patients, Alger et al. (*12*) and Fulham et al. (*13*) measured the intensity of choline signal in the tumor area in vivo. (The choline signal thus observed seems to represent the sum of all the choline-containing compounds, i.e., free choline, phosphorylcholine, glycerophosphorylcholine, phosphatidylcholine, sphingomyelin and acethylcholine (*14*).) They found the following facts:

1. The contents of choline-containing compounds are larger in brain tumor than in normal brain in most cases.
2. High-grade gliomas contain larger amounts of choline-containing compounds than do low-grade gliomas.
3. The contents of choline-containing compounds are smaller in chronic radiation necrosis than in anaplastic tumors.
4. Clinical improvement achieved by radiotherapy is followed by reduction in the content of choline-containing compounds.

These data suggest that rapidly proliferating tumors contain large amounts of membrane phospholipids, particularly phosphatidylcholine. Therefore, the direct measurement of the rate of phospholipid synthesis in human brain tumors will provide information on an aspect of phospholipid metabolism in the brain tumor.

We developed a simple method of [^{11}C]choline synthesis to be used as a radiopharmaceutical for PET of human brain tumors. After completion of animal studies, we evaluated the utility of [^{11}C]choline for the PET imaging in 24 patients with malignant brain tumor and two patients with pituitary adenoma. All of the brain tumors were visualized with PET.

MATERIALS AND METHODS

Preparation of [*methyl*-^{11}C]Choline

[^{11}C]Methyl iodide (15 GBq), prepared from $^{11}CO_2$ by Comar's method (*15*), was transferred to a conical reaction vial at 4°C and dissolved in 0.1 ml of pure (neat) dimethylaminoethanol. After the reaction vial was sealed airtight, it was heated at 120°C for 5 min. After the seal was opened, the contents of the vial were evaporated by air blow. The resulting tiny droplet of brown oil was dissolved in 5 ml of water and passed through a Sep-Pak Light Accell Plus CM cartridge (a cartridge of low capacity cation exchange resin

Received Apr. 4, 1996; revision accepted Nov. 6, 1996.
For correspondence or reprints contact: Toshihiko Hara, MD, Department of Radiology, International Medical Center of Japan, 1-21-1 Toyama, Shinjuku-ku, Tokyo 162, Japan.

with -COO^- as a functional group). After the cartridge was washed with 10 ml of water, the radioactivity of [^{11}C]choline was desorbed from the cartridge by elution with 5 ml of isotonic saline. The whole chemical procedure was performed under strictly sterile conditions and by remote-controlled operation with radiation protection.

Purity of the product was examined by reverse phase high pressure liquid chromatography (HPLC), using an Inertsil ODS-2 column (6 × 250 mm) and elution with 1 m*M* naphthalene-2-sulfonic acid + 0.05 *M* H_3PO_4 at a flow rate of 1 ml/min. The radioactivity was monitored with an ionization chamber, and the mass amount was monitored with a refractometer.

PET Study in Normal Rabbits

The time-distribution of [^{11}C]choline was studied in normal female rabbits (body weight, 2.5 kg) under Nembutal anesthesia, using PET (Headtome IV, 5-slice scanner, with 6-mm spatial resolution and 13-mm interslice interval, Shimadzu). [^{11}C]Choline (100 MBq) was bolus-injected intravenously, and the emission scan was performed across the sagittal planes repeatedly by the sequences of 1-min scan and 4-min intermission, starting at the time of injection and finishing 36 min after injection. The decay-corrected, attenuation-uncorrected PET images were reconstructed.

PET Study in Normal Human Subjects

Intracranial PET images of normal human subjects were obtained after the intravenous injection of 370 MBq of [^{11}C]choline. After a transmission scan, [^{11}C]choline was injected, then the emission scan was started at 5 min after injection. The data for the upper part of the brain (5 slices) were acquired in 5 min. Then after shifting the bed position, the data for the lower part of the brain (5 slices) were acquired for the same scanning period. By combining the two sets of the attenuation-corrected and decay-corrected PET images, the whole brain image was reconstituted.

PET Study in Patients with Brain Tumor

The clinical utility of [^{11}C]choline PET for detection of brain tumors was evaluated in 31 patients. Informed consent was given by all of the patients, and the institutional review board approved them. The data acquisition protocol for the patients was the same as for normal subjects. The radioactivity concentration in tumor within a region of interest was expressed as the concentration in tumor relative to the average radioactivity concentration in the normal cerebral tissue (tumor/normal brain [^{11}C]choline uptake ratio). Before conducting the [^{11}C]choline PET study, every patient underwent a cerebral blood flow (CBF) measurement by PET with an intravenous injection of [^{15}O]water (a 60-sec data acquisition after radioactivity emerged in the brain field) (*16*). Two separate injections of [^{15}O]water were performed, and the whole brain image was reconstituted by joining the two separate sets of images.

RESULTS

Carbon-11-Choline Preparation

In the [^{11}C]choline injection solution, HPLC showed only a single radioactive component with the retention time of 11.7 min (Fig. 1). It was identical with the retention time of an authentic choline preparation determined by refractometry. The radiochemical purity of [^{11}C]choline in the final solution was more than 98%. The radiochemical yield relative to [^{11}C]methyl iodide was more than 98% with decay correction. In the refractometry, however, another small peak was detected in the final solution; it was dimethylaminoethanol with a retention time of 11.2 min (a NaCl peak appeared at 6.8 min). The ingredient were choline, 10 μg/5 ml, and dimethylaminoethanol, less than 1 μg/5 ml. Routinely, 11 GBq of [^{11}C]choline (10 μg) was synthesized after a 10-min bombardment of 20 MeV proton at 30 μA, from 15 GBq of [^{11}C]methyl iodide. The specific activity of the [^{11}C]choline preparation was calculated as 1.1 GBq/μg (133 GBq/μmol). It took 25 min from the cyclotron start-up to the finish of the [^{11}C]choline synthesis.

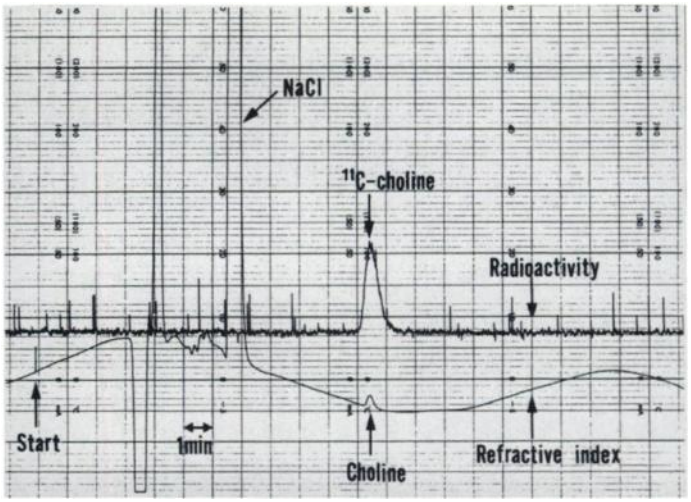

FIGURE 1. HPLC pattern of the [^{11}C]choline injection solution. Carbon-11-choline is the only radioactive component.

A sample of the reaction product taken before the passage through a Sep-Pak CM cartridge was analyzed with HPLC, giving the following result. There was only one radioactive component with the retention time of 11.7 min that was identical with that of choline. In refractometry, however, there were three components, i.e., dimethylaminoethanol detected at 11.2 min, choline at 11.7 min and an unidentified component at 16.4 min. The mass ratio between these three components was 0.1:1:10. The unidentified component was collected in the water washing (10 ml) from the Sep-Pak CM cartridge. It was a water-soluble compound, with either a neutral or negative charge and carried no radioactivity. It was possibly dimethylaminoacetic acid produced by the decomposition of dimethylaminoethanol.

The final product was the [^{11}C]choline solution dissolved in isotonic saline and was pyrogen-free when examined by the Limulus lysate test. It was ready for intravenous injection to humans. It was possible to use a single batch of [^{11}C]choline (11 GBq, initially) for the injection of two or three patients at a dose of 370 MBq each. Regarding safety, we have administered the [^{11}C]choline preparation to more than 100 human subjects and observed no adverse effect.

PET Study in Normal Rabbits

Figure 2 shows the sequential PET images of the whole body sagittal sections of a rabbit through 36 min after intravenous injection of [^{11}C]choline. At 0–1 min, radioactivity was highest in kidneys, followed by the heart-blood pool. (Heart-blood pool is visible in the upper right image in Figure 2.) The heart-blood pool image disappeared in 5 min. The liver image started to appear at 5 min and became more intense subsequently. The initial high uptake of the kidneys decreased gradually. Neither the urinary bladder nor urine were visible throughout the experiment. The pancreas and proximal portion of the small intestine were visualized. The spleen became prominent in later periods. The brain, lungs, heart (myocardium) and intrapelvic organs were not visualized in any period. At the end of this experiment, the highest uptake was in the liver, followed by the kidneys and spleen.

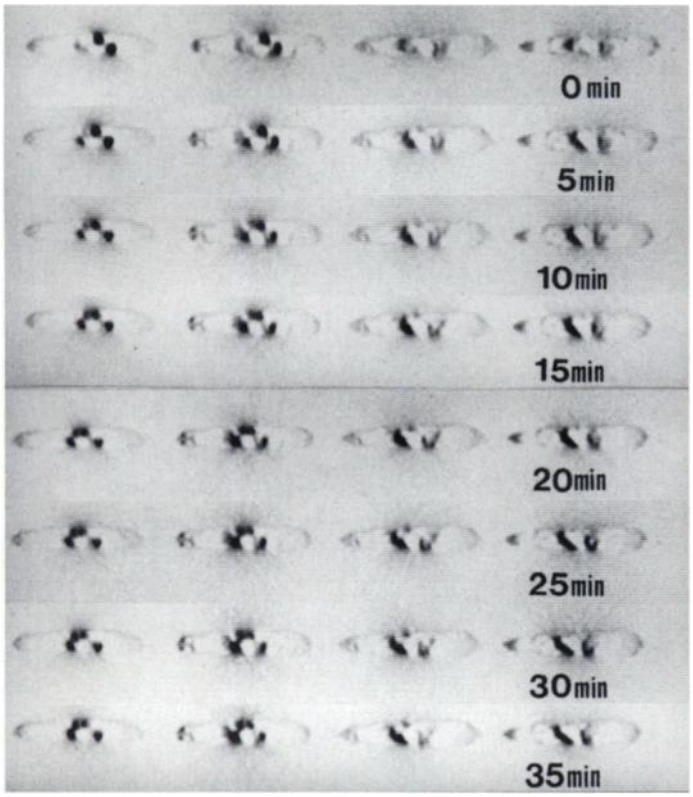

FIGURE 2. Sequential PET images of whole body sagittal sections of a rabbit after intravenous injection of [^{11}C]choline, with decay correction. In each image, left is the rostal side, and right is the caudal side. The top row (top four images) shows the data obtained at 0–1 min after injection; far left is the dorsal side, and far right is the ventral side. Each row represents the data obtained at 5-min intervals with data acquisition period of 1 min.

PET Study in Normal Human Subjects

In the preliminary study in human subjects, we found that the distribution of [^{11}C]choline in the intracranial tissues did not change with time if the radioactive decay was corrected (data not shown). Figure 3 shows PET images of normal human brain and neighboring structures, taken at 5–21 min (with a 5-min scanning for each image) after injection of [^{11}C]choline. The radioactivity in brain tissue was very low. The radioactivity in sagittal and transverse sinuses was slightly higher than in brain tissue. The radioactivity in venous plexuses, i.e., choroid plexus in lateral ventricles and plexus venosus caroticus internus, was relatively high. The pituitary body was the only organ of the brain to show high uptake. The mucous membranes of the nasal cavities showed considerably high uptake. The scalp soft tissue showed moderate uptake.

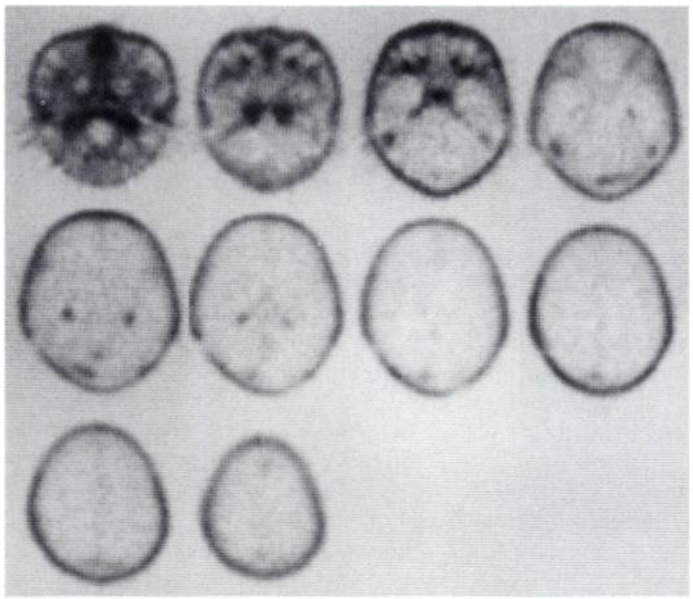

FIGURE 3. PET images of normal human brain, taken at 5–21 min (data acquisition, 5 min each) after intravenous injection of [^{11}C]choline. The uptake in the brain was very low relative to the uptake in the extracerebral tissues.

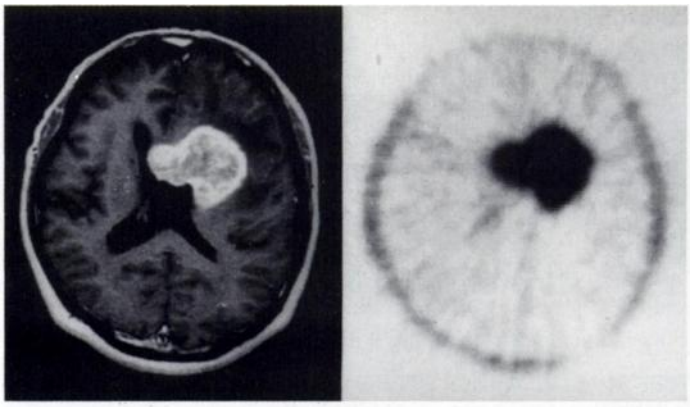

FIGURE 4. Case 1, brain tumor (glioblastoma multiforme); MRI with enhancement (left) and PET with [^{11}C]choline (right). Tumor/normal brain [^{11}C]choline uptake ratio, 13.4; tumor/normal brain CBF ratio, 1.7.

PET Study in Patients with Brain Tumor

Following are the typical results of the PET study obtained from patients with malignant brain tumors.

Case 1. A 68-yr-old man presented with right hemiparesis and stupor. Brain MRI revealed a tumor mass (5 × 4 cm), localized in the corona radiata in the left frontal lobe, extending across the corpus callosum to the right frontal lobe. The tumor was surrounded by a large edematous area in the left hemisphere. The rim of the mass, but not its center, was markedly enhanced after injection of contrast medium. Histopathological examination after stereotactic biopsy of the tumor revealed glioblastoma multiforme. The [^{11}C]choline PET was performed; [^{11}C]choline was taken up strongly in the tumor, particularly in the rim of the tumor (tumor/normal brain [^{11}C]choline uptake ratio, 13.4; tumor/normal brain CBF ratio, 1.7) (Fig. 4).

Case 2. A 56-yr-old man presented with unsteady gait and loss of appetite. MRI revealed a brain tumor (3 × 3 cm) adjoined to a cyst (4 × 3 cm) in the left cerebellum. An edematous area was noted around the tumor and cyst. Both lateral ventricles and the third ventricle were dilated. The tumor mass was enhanced homogeneously by injection of contrast medium. The [^{11}C]choline PET showed a conspicuously high uptake of [^{11}C]choline in the tumor (tumor/normal brain [^{11}C]choline uptake ratio, 27.5; tumor/normal brain CBF ratio, 2.0) (Fig. 5A). A few days later, the tumor and cyst were resected surgically. The pathological diagnosis was hemangioblastoma. One month later, MRI with contrast medium showed a relatively large (3 × 3 cm) high intensity area in the surgically defected area. The [^{11}C]choline PET, performed shortly after, revealed no abnormal uptake in this area (Fig. 5B).

Case 3. A 76-yr-old man presented with left hemiparesis and memory deficit. Brain CT revealed a contrast-enhanced mass in the right parietal cortex of the brain (2 × 2 cm) surrounded by a very large edematous area. Chest CT showed an abnormal mass in the right upper lobe and an enlarged lymph node on the bronchial carina. It was determined as adenocarcinoma histopathologically. The abnormal mass in the brain was regarded as a metastatic tumor originating in the lung. Radiotherapy with 30 Gy was delivered to the right cerebrum, alleviating the brain

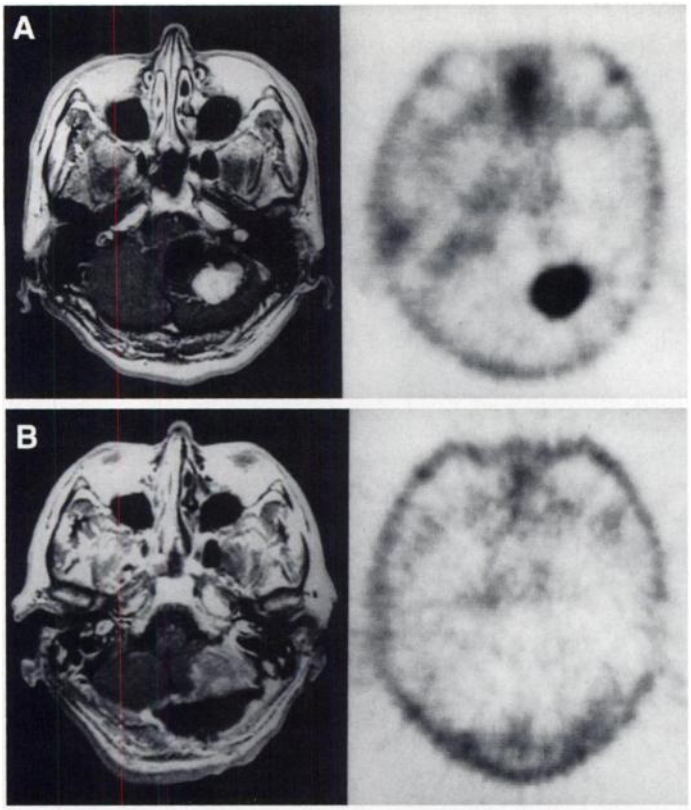

FIGURE 5. Patient 2 with a brain tumor (hemangioblastoma). (A) MRI with enhancement (left) and PET with [^{11}C]choline (right). Tumor-to-normal brain [^{11}C]choline uptake ratio, 27.5; tumor-to-normal brain CBF ratio, 2.0. (B) Same patient after resection of the brain tumor. MRI with enhancement (left) and PET with [^{11}C]choline (right).

edema but with no effect on the tumor size. The [^{11}C]choline PET scan of the brain was performed during this period, with the brain tumor demonstrating a markedly high uptake of [^{11}C]choline (tumor/normal brain [^{11}C]choline uptake ratio, 10.7; tumor/normal brain CBF ratio, 0.9) (Fig. 6).

Cumulated Case Studies

Table 1 shows the cumulated data we obtained from the combination of [^{11}C]choline PET and [^{15}O]water PET (CBF) in patients with brain tumor and other brain diseases.

[^{11}C]Choline PET always gave high uptake (positive) images of the malignant brain tumor (24 cases) and pituitary adenoma (two patients) surrounded by a background of very low radioactivity. The blood flow rate in the tumor measured by

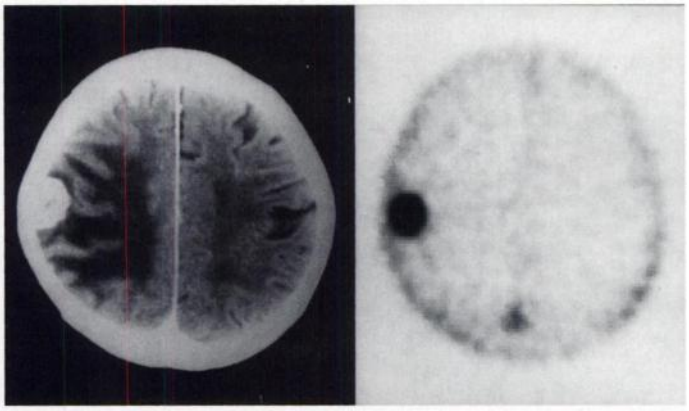

FIGURE 6. Patient 3 with a brain tumor caused by metastasis of lung cancer (adenocarcinoma) CT with enhancement (left) and PET with [^{11}C]choline (right). Tumor-to-normal brain [^{11}C]choline uptake ratio, 10.7; tumor-to-normal brain CBF ratio, 0.9.

TABLE 1
Cumulated Data Obtained from [^{11}C]Choline and [^{15}O]Water (CBF) PET in Patients with Brain Tumor and Other Brain Diseases

Diagnosis	[^{11}C]Choline*	[^{15}O]Water†	No. of patients
Brain tumor (malignant)	Positive	Increased	6
	Positive	Unchanged	4
	Positive	Decreased	14
Pituitary adenoma	Positive	Unchanged	1
	Positive	Decreased	1
Brain infarct or hemorrhage	Negative	Decreased	4
Meningitis (tuberculous)	Positive	Increased	1

*The [^{11}C]choline uptake in lesions was evaluated as positive if the uptake was markedly higher than in normal brain tissue and negative if the uptake was far less than in normal brain tissue.

†CBF in lesions was evaluated as increased, unchanged or decreased in comparison with the blood flow in normal brain tissue.

[^{15}O]water PET was expressed as increased, unchanged or decreased in relation to the blood flow rate in normal brain tissue. The degree of [^{11}C]choline uptake in the brain tumor was independent of the blood flow rate in the tumor. In all of the malignant brain tumor patients, there was no difference in [^{11}C]choline uptake between the brain edema and the normal brain tissue.

Pituitary adenoma (two patients) was visualized by [^{11}C]choline PET, although normal pituitary body takes up [^{11}C]choline, also.

Cerebrovascular disease, i.e., cerebral infarct and hemorrhage (four patients), showed no uptake of [^{11}C]choline.

One patient with tuberculous meningitis showed a considerably high uptake of [^{11}C]choline in various areas of the subarachnoidal space ([^{18}F]FDG PET did not show uptake in the corresponding area).

DISCUSSION

We have developed a simple method of [*methyl*-^{11}C]choline synthesis. The characteristic of this synthetic method is the use of "neat" dimethylaminoethanol, which dissolves [^{11}C]methyl iodide and reacts with [^{11}C]methyl iodide directly; there was no need to use additional solvent nor the need to use supplemental strong base. The purification was simply conducted by evaporation of substrates and use of a disposable ion-exchange cartridge.

Fluorine 18-FDG and ^{11}C-methionine PET are widely used clinically for evaluation of patients with brain tumors (*17–22*). The purpose of these studies are:

1. to accurately delineate the extent of tumors at the time of diagnosis,
2. to provide information related to prognosis,
3. to distinguish between the brain damage and the tumor persistence after resection or radiation of the tumor, and
4. to detect progression or recurrence of the tumor.

Carbon-11-methionine is superior to [^{18}F]FDG in properly delineating the border of brain tumors in the PET image because the activity of [^{18}F]FDG in brain tumors is either higher or lower than the activity in normal brain tissue obscuring the tumor border depending on the glucose metabolic rate of the tumor (*21*). We developed the [^{11}C]choline PET method as another means to clearly visualize the brain tumors.

Carbon-11-choline PET gave better images of brain tumors than did [^{11}C]methionine PET (data not shown) because the tumor-to-background ratio was higher with [^{11}C]choline PET

because of the lower background. Carbon-11-choline PET had another advantage over [^{11}C]methionine PET in brain tumor imaging because the metabolism of [^{11}C]choline in brain tumors is simple, i.e., mainly directed to phospholipid synthesis (*5–9*), and therefore the interpretation of the image is straightforward. This is in contrast to the complex metabolism of [*methyl*-^{11}C]methionine; one is directed for the protein synthesis and the other for the integration of *methyl*-^{11}C group into various molecules (transmethylation) (*23*); the donation of the methyl group to phosphatidylcholine (via *S*-adenosylmethionine) is an example of the transmethylation reaction (*24,25*). The [^{11}C]methionine PET represents the sum of the above two reaction pathways. Ishiwata et al. (*26*) reported that, after injection of [*methyl*-^{3}H]methionine to tumor-bearing mice, significant fractions of radioactivity found in brain and tumor were in nonprotein substances such as lipids and RNA and that the tissue uptake increased by the treatment with protein synthesis inhibitor, cycloheximide. Recently, Ishiwata et al. (*27*) also showed that the [*methyl*-^{11}C]methionine uptake in liver of mice was mainly involved with phospholipid synthesis through the transmethylation reaction.

Carbon-11-choline PET was superior to [^{18}F]FDG PET for brain tumor imaging because [^{11}C]choline PET always gives clearer images of brain tumors, whereas [^{18}F]FDG PET does not always delineate the border of the tumor. The high uptake of [^{18}F]FDG in the normal brain tissue frequently obscures the tumor uptake. Carbon-11-choline PET had an additional but very important advantage over [^{18}F]FDG PET in the brain tumor imaging. With [^{11}C]choline, the emission scan can be started at 5 min after injection, since the blood clearance is very rapid and the radioactivity distribution in tissues becomes almost constant in 5 min. On the contrary, with [^{18}F]FDG, it takes 40–60 min after injection before the emission scan can be started; this period is too long for both the patient and the staff, and it also hampers the running efficiency of the PET scanner.

Haubrich et al. (*1*) studied the distribution and metabolism of intravenously administered [*methyl*-^{3}H]choline in various tissues of guinea pigs. They observed that [^{3}H]choline in blood declined very rapidly, and its plasma concentration at 2 min after injection was 1/100 of the initial plasma concentration. The organs that showed the highest uptake were the kidney and liver; the sum of the uptake dose in these organs was 50% of the administered dose, at 3 min. There was a 30-fold difference in the uptake rate for various organs in the following order: kidney $\gg$ liver > lung > submaxillary gland > duodenum > fat > heart $\gg$ cerebral cortex. The radioactivity in urine was negligible. At 60 min after administration of [^{3}H]choline, most of the radioactivity in the tissues was found in various fractions of choline metabolites. The radioactivity in the cerebral cortex at 60 min was 1.3% in acetylcholine fraction, 64% in phosphorylcholine fraction and 23% in lipid fraction. The majority of radioactivity in blood plasma at 60 min was found in the betaine fraction.

It is known that conversion of choline to betaine occurs rapidly in kidneys (*28,29*) and at a lesser rate in liver (*30–32*); betaine is further used for the transmethylation reaction to form methionine (*33*).

We observed that the uptake of [^{11}C]choline in normal brain tissue was very low, confirming the previous reports of Haubrich et al. (*1*) and Friedland et al. (*2*). The low uptake in normal brain was in sharp contrast to the high uptake in nasal mucosa and venous plexus in the [^{11}C]choline PET image.

Svane-Knudsen et al. (*34*) found in electron microscopy of the human nasal wall that some of the cells in mucosal glands contain granules resembling lamellar bodies of the type II alveolar cells of normal lung. Type II alveolar cells are known to produce pulmonary surfactants, of which the major constituent is phosphatidylcholine (*35,36*). This fact may explain why [^{11}C]choline accumulated so markedly in nasal mucosa in our study.

In addition, it is well known from in vitro studies that choline accumulates in the endothelium of cerebral blood vessels (*37–40*). This may also explain why [^{11}C]choline accumulated in the choroid plexus in lateral ventricles and plexus venosus caroticus internus in our human study.

The most pertinent observation in this study was the very high uptake of [^{11}C]choline in brain tumors. We obtained positive tumor images with [^{11}C]choline in 24 patients. The great difference in the [^{11}C]choline uptake between brain tumor and normal brain tissue provided clearly delineated tumor images. The high uptake of [^{11}C]choline in brain tumors seemed to have relevance to the observation made in cultured neurogenic tumor cells; radioactive choline is rapidly incorporated into tumor cells, then phosphorylated to become phosphorylcholine (analogously to FDG phosphorylation) and finally integrated into a phospholipid, i.e., phosphatidylcholine (*6–9*). This high uptake also seemed related to the MRS findings, in which high content of choline-containing compounds was found in the brain tumors (*12,13*).

Finally, a comment is needed on the chemical species that gives rise to the choline signal in vivo in MRS. Peeling and Sutherland (*41*) and Urenius et al. (*42*) studied the concentration of choline-containing compounds in perchloric acid extracts of human brain tumors by in vitro ^{1}H MRS. They did not find any change in the content of acid-extractable choline-containing compounds in brain tumors other than pituitary adenomas. Nevertheless, Urenius et al. (*42*) found in the above study that the signal of choline-containing compounds of low-grade gliomas was increased in vivo. It is likely, therefore, that the increased choline signal observed in vivo has come from the acid-insoluble membrane phospholipids, particularly phosphatidylcholine.

Kugel et al. (*43*) found large choline MRS signals in vivo in slowly growing meningiomas. It is possible that our [^{11}C]choline would also be incorporated strongly in this tumor type.

ACKNOWLEDGMENTS

This work was supported in part by the Science and Technology Agency of Japan and the Japanese Smoking Research Foundation.

REFERENCES

1. Haubrich DR, Wang PFL, Wedeking PW. Distribution and metabolism of intravenously administered choline[methyl-^{3}H] and synthesis in vivo of acetylcholine in various tissues of guinea pigs. *J Pharmacol Exp Ther* 1975;193:246–255.
2. Friedland RP, Mathis CA, Budinger TF, Moyer BR, Rosen M. Labeled choline and phosphorylcholine: body distribution and brain autoradiography: concise communication. *J Nucl Med* 1983;24:812–815.
3. Gauthier S, Diksic M, Yamamoto L, Tyler J, Feindel W. Positron emission tomography with [^{11}C]choline in human subjects. *Can J Neurol Sci* 1985;12:214.
4. Ishidate K. Choline transport and choline kinase. In: Vance DE, ed. *Phosphatidylcholine metabolism.* Boca Raton, Florida: CRC Press; 1989:9–32.
5. Yavin E. Regulation of phospholipid metabolism in differentiating cells from rat brain cerebral hemispheres in culture: patterns of acetylcholine, phosphocholine and choline phosphoglycerides labeling from [*methyl*-^{14}C]choline. *J Biol Chem* 1976;251:1392–1397.
6. Lanks K, Somers L, Papirmeister B, Yamamura H. Choline transport by neuroblastoma cells in tissue culture. *Nature* 1974;252:476–478.
7. Liscovitch M, Slack B, Blusztain JK, Wurtman RJ. Differential regulation of phosphatidylcholine biosynthesis by 12-O-tetradecanoylphorbol-13-acetate and diacylglycerol in NG108–15 neuroblastoma × glioma hybrid cells. *J Biol Chem* 1987; 262:17487–17491.
8. George TP, Morash SC, Cook HW, Byers DM, Palmer FBStC, Spence MW. Phosphatidylcholine biosynthesis in cultured glioma cells: evidence for channeling of intermediates. *Biochim Biophys Acta* 1989;1004:283–291.
9. Yorek MA, Dunlap JA, Spector AA, Ginsberg BH. Effect of ethanolamine on choline uptake and incorporation into phosphatidylcholine in human Y79 retinoblastoma cells. *J Lipid Res* 1986;27:1205–1213.

10. Slack BE, Richardson U, Nitsch RM, Wurtman RJ. Dioctanoylglycerol stimulates accumulation of [methyl-^{14}C]choline and its incorporation into acetylcholine and phosphatidylcholine in a human cholinergic neuroblastoma cell line. *Brain Res* 1992;585:169–176.
11. Pardridge WM. Transport of nutrients and hormones through the blood-brain barrier. *Fed Proc* 1984;43:201–204.
12. Alger JR, Frank JA, Bizzi A, et al. Metabolism of human gliomas: assessment with H-1 MR spectroscopy and F-18 fluorodeoxyglucose PET. *Radiology* 1990;177:633–641.
13. Fulham MJ, Bizzi A, Dietz MJ, et al. Mapping of brain tumor metabolites with proton MR spectroscopic imaging: clinical relevance. *Radiology* 1992;185:675–686.
14. Miller BL. A review of chemical issues in ^{1}H NMR spectroscopy: N-acetyl-L-aspartate, creatine and choline. *NMR Biomed* 1991;4:47–52.
15. Comar D, Cartron JC, Maziere M, Marazano C. Labeling and metabolism of methionine-methyl-^{11}C. *Eur J Nucl Med* 1976;1:11–14.
16. Fox PT, Mintun MA. Noninvasive functional brain mapping by change-distribution analysis of averaged PET images of $H_2{}^{15}O$ tissue activity. *J Nucl Med* 1989;30:141–149.
17. Coleman RE, Hoffman JM, Hanson MW, Sostman HD, Schold SC. Clinical application of PET for the evaluation of brain tumors. *J Nucl Med* 1991;32:616–622.
18. Janus TJ, Kim EE, Tilbury R, Bruner JM, Yung WKF. Use of [^{18}F]fluorodeoxyglucose positron emission tomography in patients with primary malignant brain tumors. *Ann Neurol* 1993;33:540–548.
19. Glantz MJ, Hoffman JM, Coleman RE, et al. Identification of early recurrence of primary central nervous system tumors by [^{18}F]fluorodeoxyglucose positron emission tomography. *Ann Neurol* 1991;29:347–355.
20. Derlon JM, Bourdet C, Bustany P, et al. [^{11}C]L-Methionine uptake in gliomas. *Neurosurgery* 1989;25:720–728.
21. Ogawa T, Kanno I, Shishido F, et al. Clinical value of PET with ^{18}F-fluorodeoxyglucose and L-methyl-^{11}C-methionine for diagnosis of recurrent brain tumor and radiation injury. *Acta Radiol* 1991;32:197–202.
22. Ogawa T, Hatazawa J, Inugami A, et al. Carbon-11-methionine PET evaluation of intracerebral hematoma: distinguishing neoplastic from non-neoplastic hematoma. *J Nucl Med* 1995;36:2175–2179.
23. Barrio JR. Biochemical principles in radiopharmaceutical design and utilization. In: Phelps ME, Mazziotta JC, Schelbert HR, eds. *Positron emission tomography and autoradiography: principles and applications for the brain and heart.* New York: Raven Press; 1986:451–492.
24. Maziere C, Maziere JC, Mora L, Polonovski J. Early increase in phosphatidylcholine synthesis by choline and transmethylation pathways in spreading fibroblasts. *Exp Cell Res* 1986;167:257–261.
25. Lakher MB, Wurtman RJ. Molecular composition of the phosphatidylcholines produced by the phospholipid methylation pathway in rat brain in vivo. *Biochem J* 1987;244:325–330.
26. Ishiwata K, Kubota K, Murakami M, et al. Re-evaluation of amino acid PET studies: can the protein synthesis rates in brain and tumor tissues be measured in vivo? *J Nucl Med* 1993;34:1936–1943.
27. Ishiwata K, Enomoto K, Sasaki T, et al. A feasibility study on L-[1-carbon-11]tyrosine and L-[methyl-carbon-11]methionine to assess liver protein synthesis by PET. *J Nucl Med* 1996;37:279–285.
28. Eng J, Berkowitz BA, Balaban RS. Renal distribution and metabolism of [$^{2}H_9$]choline. A ^{2}H NMR and MRI study. *NMR Biomed* 1990;3:173–177.
29. Grossman EB, Hebert SC. Renal inner medullary choline dehydrogenase activity: characterization and modulation. *Am J Physiol* 1989;256:107–112.
30. Zeisel SH, Story DL, Wurtman RJ, Brunengraber H. Uptake of free choline by isolated perfused rat liver. *Proc Natl Acad Sci USA* 1980;77:4417–4419.
31. Pritchard PH, Vance DE. Choline metabolism and phosphatidylcholine biosynthesis in cultured rat hepatocytes. *Biochem J* 1981;196:261–267.
32. Pelech SL, Pritchard PH, Vance DE. Prolonged effects of cyclic AMP analogs on phosphatidylcholine biosynthesis in cultured rat hepatocytes. *Biochem Biophys Acta* 1982;713:260–269.
33. Storch KJ, Wagner DA, Young VR. Methionine kinetics in adult men: effect of dietary betaine on L-[$^{2}H_3$-methyl-1-^{13}C]methionine. *Am J Clin Nutr* 1991;54:386–394.
34. Svane-Knudsen V, Rasmussen G, Clausen PP. Surfactant-like lamellar bodies in the mucosa of the human nose. *Acta Otolaryngol* 1990;109:307–313.
35. Snyder F, Malone B. Acyltransferases and the biosynthesis of pulmonary surfactant lipid in adenoma alveolar type II cells. *Biochem Biophy Res Commun* 1975;66:914–919.
36. Rooney SA. The surfactant system and lung phospholipid biochemistry. *Am Rev Respir Dis* 1985;131:439–460.
37. Arneric SP, Honig MA, Milner TA, Greco S, Iadecola C, Reis DJ. Sites of acetylcholine synthesis and release associated with microvessels in cerebral cortex: ultrastructural and neurochemical studies. *J Cereb Blood Flow Metab* 1987;7:S330.
38. Hamel E, Assumel-Lurdin C, Edvinsson L, Fage D, MacKenzie ET. Neuronal versus endothelial origin of vasoactive acethylcholine in pial vessels. *Brain Res* 1987;420:391–396.
39. Estrada C, Bready J, Berliner J, Cancilla PA. Choline uptake by cerebral capillary endothelial cells in culture. *J Neurochem* 1990;54:1467–1473.
40. Galea E, Estrada C. Ouabaine-sensitive choline transport system in capillaries isolated from bovine brain. *J Neurochem* 1992;59:936–941.
41. Peeling J, Sutherland G. High-resolution ^{1}H NMR spectroscopy studies of extracts of human cerebral neoplasms. *Magn Reson Med* 1992;24:123–136.
42. Usenius JPR, Kauppinen RA, Vainio PA, et al. Quantitative metabolite patterns of human brain tumors: detection by ^{1}H NMR spectroscopy in vivo and in vitro. *J Comput Assist Tomogr* 1994;18:705–713.
43. Kugel H, Heindel W, Ernestus RI, et al. Human brain tumors: spectral patterns detected with localized H-1 MR spectroscopy. *Radiology* 1992;183:701–709.

Comparison of Copper-67- and Iodine-125-Labeled Anti-CEA Monoclonal Antibody Biodistribution in Patients with Colorectal Tumors

Angelika Bischof Delaloye, Bernard Delaloye, Franz Buchegger, Charles-André Vogel, Michel Gillet, Jean-Pierre Mach, Alan Smith and P. August Schubiger

Departments of Nuclear Medicine and Surgery, Institute of Biochemistry, University of Lausanne, Lausanne; and Division of Radiopharmacy, Paul Scherrer Institute, Villigen, Switzerland

Copper-67 has comparable beta-particle emissions to that of ^{131}I, but it displays more favorable gamma emission characteristics for application in radioimmunotherapy (RIT). This study investigates the potential of ^{67}Cu-labeled monoclonal antibody (MAb) 35 for RIT of colorectal carcinoma. **Methods:** Biokinetics of simultaneously injected ^{67}Cu- and ^{125}I-labeled MAb35 were studied in six patients scheduled for surgery of primary colorectal cancer. **Results:** Whole-body clearance ($T_{1/2}$) of ^{67}Cu, estimated from sequential anterior and posterior whole-body scans and corrected for decay of ^{67}Cu, was 41 hr. Serum clearance of ^{67}Cu was faster (27.41 hr) than that of ^{125}I (38.33 hr). Mean tumor uptake of the ^{67}Cu-labeled compound (0.0133 %ID/g) exceeded that of ^{125}I (0.0095 %ID/g), and tumor-to-blood ratios were higher for ^{67}Cu than for ^{125}I, with averages of 6.07 and 2.41, respectively. The average ^{67}Cu/^{125}I ratio was 1.9 for tumor uptake, 0.7 for blood and 2.6 for tumor-to-blood ratios. Nonspecific liver uptake of ^{67}Cu as calculated from whole-body scans was high in four patients, up to 25% of residual whole-body activity at 48 hr, but did not increase with time. We also observed some nonspecific bowel activity, as well as moderate to high uptake in benign polyps. **Conclusion:** Copper-67-labeled MAb35 is more favorable than its radioiodine-labeled counterpart for RIT of colorectal carcinoma due to higher tumor-to-blood ratios, but the problem of nonspecific liver and bowel uptake must first be overcome. The absolute accumulation of activity in tumor remains low, however, so the probability of cure with this compound alone is questionable. The use of ^{67}Cu as one component of a multimodality adjuvant treatment seems to remain the most appropriate application for RIT.

Key Words: anti-CEA; monoclonal antibodies; radioimmunotherapy; copper-67; iodine-125; colorectal carcinoma

J Nucl Med 1997; 38:847–853

Received May 13, 1996; revision accepted Nov. 6, 1996.

For correspondence or reprints contact: Angelika Bischof Delaloye, MD, Nuclear Medicine Department, Centre Hospitalier Universitaire Vaudois, CH-1011 Lausanne, Switzerland.

Most radioimmunotherapy (RIT) trials have been performed with ^{131}I-labeled monoclonal antibodies (MAb) (*1–11*). Despite advantages such as low price, extensive experience with ^{131}I in